

# Weierstrass scale space representation and composite dilated U-net based convolution for early glaucoma diagnosis

Abdul Basith Zahir Hussain<sup>1</sup>, Sulthan Ibrahim Mohamed Sulaiman<sup>2</sup>

<sup>1</sup>Department of Computer Application, Madurai Kamaraj University (MKU), Madurai, India

<sup>2</sup>Department of Computer Science, Government Arts and Science College, Theni, India

## Article Info

### Article history:

Received May 14, 2024

Revised Nov 12, 2024

Accepted Nov 24, 2024

### Keywords:

Composite dilated U-net based convolution

Deep learning

Glaucoma detection

Scale space representation

Weierstrass transform

## ABSTRACT

Glaucoma is one of the common causes of blindness in the current world. Glaucoma is a blinding optic neuropathy characterized by the degeneration of retinal ganglion cells (RGCs). Accurate diagnosis and monitoring of glaucoma are challenging task through eye examinations and additional tests. To achieve accurate diagnosis of glaucoma with higher sensitivity and specificity, novel method called Weierstrass scale space representation and composite dilated U-net based convolution (WSSR-CDC) is introduced. At first, the Weierstrass transform scale space representation is employed to enhance image structures at various scales with higher accuracy of region of interest (ROI) detection using Euler's identity. Next, CDC model is utilized with several layers. In input layer, preprocessed input images are taken as input. Fragment derivative are formulated for every preprocessed input. Log cosh dice loss function and optic cup to disc ratio are computed for segmented glaucoma detected results. With this, the accurate diagnosis of glaucoma is made with minimal error. The WSSR-CDC method was evaluated using the glaucoma fundus imaging dataset with several factors. The results show that the WSSR-CDC method outperforms conventional techniques, improving accuracy by 24% and sensitivity by 18%. It demonstrates promising results in fast, accurate, diagnosis of glaucoma.

This is an open access article under the [CC BY-SA](https://creativecommons.org/licenses/by-sa/4.0/) license.



## Corresponding Author:

Abdul Basith Zahir Hussain

Department of Computer Application, Madurai Kamaraj University (MKU)

Madurai, 625 021 Tamil Nadu, India

Email: abdbasith93@gmail.com

## 1. INTRODUCTION

One of the paramount sources of blindness creating optic nerve damage is glaucoma. If undiagnosed timely, glaucoma brings about irreversible destruction to the optic nerve resulting in blindness. Usually, ophthalmologists conduct disease diagnosis through retinal scrutiny of broadened pupils by means of segmentation. Machine learning techniques, hitherto now being steered and vigorous necessitates automated solutions. The optic nerve head inspection that necessitates quantification of cup-to-disc ratio (CDR) is contemplated as the most pertinent technique of glaucoma disease diagnosis. Owing to this, deep learning (DL) techniques as a consequence of self-learning can institute automated diagnostic courses of actions in minimal time. Contrast limited adaptive histogram equalization (CLAHE) was utilized as a preprocessing step in multi-feature deep learning (MFDL) was developed by Xue *et al.* [1] to carry on comparison images compatible as well as regularize clarification across images in the database therefore improving true positive rate of glaucoma detection. However, image structures are different scales was not focused, therefore compromising the accuracy of region of interest (ROI) detection. A new multi-task DL method which influences correlations of associated eye-fundus tasks and quantifications utilized in glaucoma analysis was

presented by Pascal *et al.* [2]. With this the probability that the method ranked a random positive sample was more than a random negative sample, therefore improve the area under the receiver operating characteristic (ROC) curve significantly. However, with the sparse potentiality in segmenting edge features and inadequate extraction of position information, therefore causing image diagnostic errors.

The above conventional methods are illustrated in major problems including minimum accuracy, higher error, and failure to provide accurate glaucoma detection and sensitivity and specificity were not considered. Forementioned issues and results factor, in this work a method called, Weierstrass scale space representation and composite dilated U-Net based convolution (WSSR-CDC) for glaucoma detection is introduced. To improve sensitivity as well as specificity of glaucoma recognition, to aid in differentiating true pathology from normal variability, the WSSR-CDC technique is designed. WSSR-CDC technique is developed through preprocessing and segmentation on contrary to conventional work which employs normalizing the illumination across the images.

The rest of the paper is ordered as follows. Section 2 portrays the related works. In section 3, the methodology of research is detailed. The experimental settings are provided and implementation details are presented in section 4. In section 4, the result analysis is discussed. Finally, section 5 describes the conclusion of the paper.

## 2. LITERATURE SURVEY

A DL algorithm employing convolutional neural network (CNN) based glaucoma detection to focus on the diagnostic error was presented by Kim *et al.* [3]. However, the memory consumed in storing the intermediate classified results was found to be higher. To focus on this issue, a CNN-based fully automated mechanism for glaucoma detection was presented by Saha *et al.* [4]. Despite improvement in terms of glaucoma detection, the time consumption was not focused. However, early glaucoma detection can even stop the vision loss. With this objective two phases focusing localization via optic disc and accordingly diagnosing glaucoma via network model was presented by Latif *et al.* [5]. Through this kind of localization method ensured accuracy but also minimized the computation cost in an extensive manner. Deep neural network has brought about encouraging results for detection of glaucoma in an automatic manner fundus images. However, the inherent inconsistency across glaucoma datasets is demanding for data-driven neural network mechanisms. This inconsistency results in the domain gap that influences model performance and decreases model generalization potentiality. Yan *et al.* [6], a mix up domain adaptation mechanism was designed that traverses' domain adaptation with domain mixup with the purpose of enhancing the overall model performance across different glaucoma datasets. However, another technique to focus on sensitivity as well as specificity employing logistic regression-based model was designed by Thanki [7] for efficient retinal fundus classification. Conventional diagnostic methods are found to be laborious and time consuming and frequently inaccurate, hence making glaucoma diagnosis in an accurate manner. To bridge this gap an automated glaucoma stage classification method employing pre-trained deep CNN model and classifier fusion. With this model not only accuracy was ensured but also resulted in early recognition. Review of DL methods was examined by Velpula and Sharma [8] for early glaucoma detection. Glaucoma detection manually is demanding part which needs proficiency as well as years of experience. Ajitha *et al.* [9], a dominant and precise algorithm employing a CNN for automatic diagnosis of glaucoma was proposed. By employing this DL technique improved the sensitivity and specificity in an extensive manner. Performance assessment of several DL techniques in predicting glaucoma via three distinct optimization algorithms was proposed by Singh *et al.* [10].

However, prevailing methods chiefly depend on a substantial amount of labeled data that is a demanding constraint for glaucoma detection. To address on this aspect, transfer induced attention network (TIA-Net) was presented by Xu *et al.* [11] for automatic glaucoma detection. People agonizing as of glaucoma frequently not observe some modify in vision at premature phases. Nevertheless, with its progression, glaucoma specifically results in vision loss that is also found to be irreversible in several cases. As a result, early diagnosis is of critical importance. Also obtaining accurate insights are also found to be a time-consuming process. D'Souza *et al.* [12], parameter-effective AlterNet-K method taking into consideration alternating design pattern integrating residual networks (ResNets) as well as multi-head self-attention (MSA) was proposed. By employing this integration model resulted in the overall improvement in generalization. Despite improvement in generalization accuracy was not focused. An ensemble of selection methods was proposed by Pathan *et al.* [13] using directional filter and dynamic selection techniques. It enhanced in general sensitivity in an extensive method. Preceding research works have shown that owing to missed diagnosis the likelihood of progression from ocular hypertension to unilateral vision loss is increasing gradually. Due to this, early glaucoma diagnosis is essential to ward off disease progression and vision loss. A combined CNN and recurrent neural network (RNN) were designed by Gheisari *et al.* [14] that through aid

of both spatial and temporal features enhanced early glaucoma detection. Yet another automated mechanism employing CNN was proposed by Schuster *et al.* [15] with improved sensitivity and specificity. However diagnostic error was not considered. Human vision has motivated notable developments in computer vision however, the human is said to be highly susceptible to several silent eye diseases. With the evolution of DL techniques, computer vision for human eye disease detection has received importance but most research work has concentrated on a constrained number of eye diseases. A two-phase localization via ODGNet was designed Latif *et al.* [16]. Also, by employing the saliency map resulted in the minimization of computation cost significantly.

CDR was measured by Sevastopolsky *et al.* [17] employing U-net CNN that in turn reduced the prediction time considerably. Yet another method to boost the learning efficiency employing D-S evidence theory was presented by Du *et al.* [18] that in turn improved recognition capability. A multi-feature analysis was performed by Akter *et al.* [19] using logistic regression to focus on the accuracy aspect. Glaucoma is the principal a leading inducement of irreversible blindness globally, influencing millions of people. Early diagnosis is crucial to minimize visual loss and numerous methods are utilized for detection of glaucoma. Puchaicela-Lozano *et al.* [20], hybrid technique for glaucoma fundus image localization employing pre-trained R-CNN as well as segmentation employing C2D area was presented. By employing the cup-to-disk area for segmentation resulted in an improvement of accuracy. Yet another transformative approach to glaucoma detection employing CNN was investigated by Haja and Mahadevappa [21]. As glaucoma materializes in later stages and it is a slow disease, detailed screening and detection is essential to keep away from vision forfeiture. Mahum *et al.* [22], for detecting glaucoma at early stages using DL-based feature extraction was presented. Challenges in artificial intelligence for glaucoma detection were investigated by Huang *et al.* [23]. Human’s grading was simulated with DL by Lin *et al.* [24] employing automated diagnosing mechanism. With this type of simulation enhanced clinical glaucoma diagnosis. Multimodal dataset was employed by Li *et al.* [25].

**3. METHOD**

Glaucoma is a disease which concern optic nerve caused through abnormally high pressure at the eye and is also considered as one of the major sources of blindness for people irrespective of the age, more frequent in older adults. Glaucoma increases CDR, exerting influence on peripheral vision loss. Accurate and precise glaucoma detection in digital fundus images is however an open topic as far as biomedical image processing is concerned. Hence, early glaucoma detection in retinal fundus image is crucial for circumventing from the vision loss. In this work a method called, WSSR-CDC is designed.

As illustrated in Figure 1, the proposed WSSR-CDC method. The input images are obtained from the glaucoma fundus image dataset. The sample images are then subjected to preprocessing and segmentation employing WSSR-CDC. Initially, preprocessing is performed by applying WSSR to generate scale-invariant preprocessed images with higher sensitivity. Second, the preprocessed sample images are subjected to a segmentation model called, CDC with various layers such as input, hidden, and output layers. Preprocessed input images are considered as input in the input layer. These layers are sent to the hidden layer. Fragment rectified linear unit (FReLU) activation and sigmoid function are employed in the hidden layer. Next, in the output layer, diagnostic error is minimized via the log cosh dice loss function. The optic CDR is determined for segmented glaucoma detected results. With this convolution model improved ROI detection is ensured in an accurate and precise manner. This process of the WSSR-CDC is explained in the following subsections.

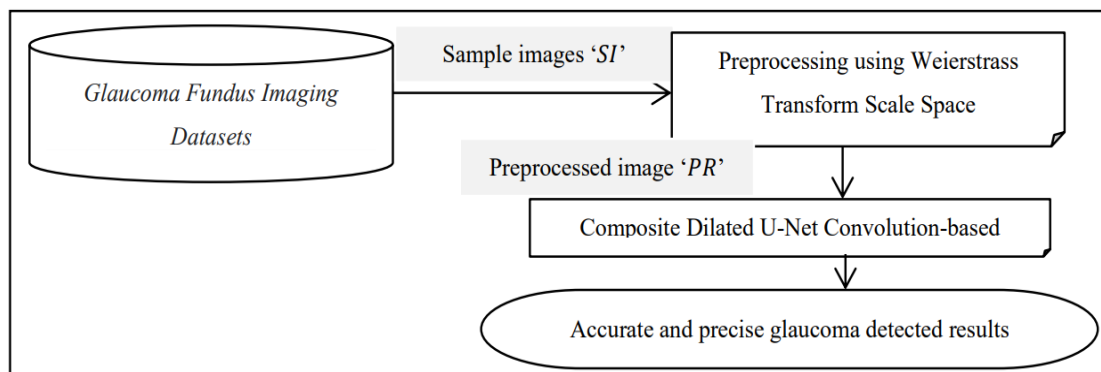


Figure 1. Block diagram of WSSR-CDC

### 3.1. Weierstrass transform scale space representation-based preprocessing

In the region of image analysis as well as disease diagnosis, the conception of scale space representation (SSR) is utilized for processing image information at numerous scales and to be more specific enhance image aspects. Special kind of SSR is given through Weierstrass approximation, wherever image information is subjected to convolution through gaussian function. The majority of theory for Weierstrass approximation scale space contract through continuous images, considering that single as executing this contain to face detail which mainly measurement information is discrete. Therefore, this Weierstrass approximation scale space contract solves the issue to discretize continuous images as preserving which leads to the selection of Weierstrass transform scale space representation-based preprocessing model. The Weierstrass transform scale space representation not only improves the image structures at different scales but also enhances the accuracy of ROI detection considerably via Euler's identity. Figure 2 shows the structure of the Weierstrass transform scale space representation-based preprocessing model.

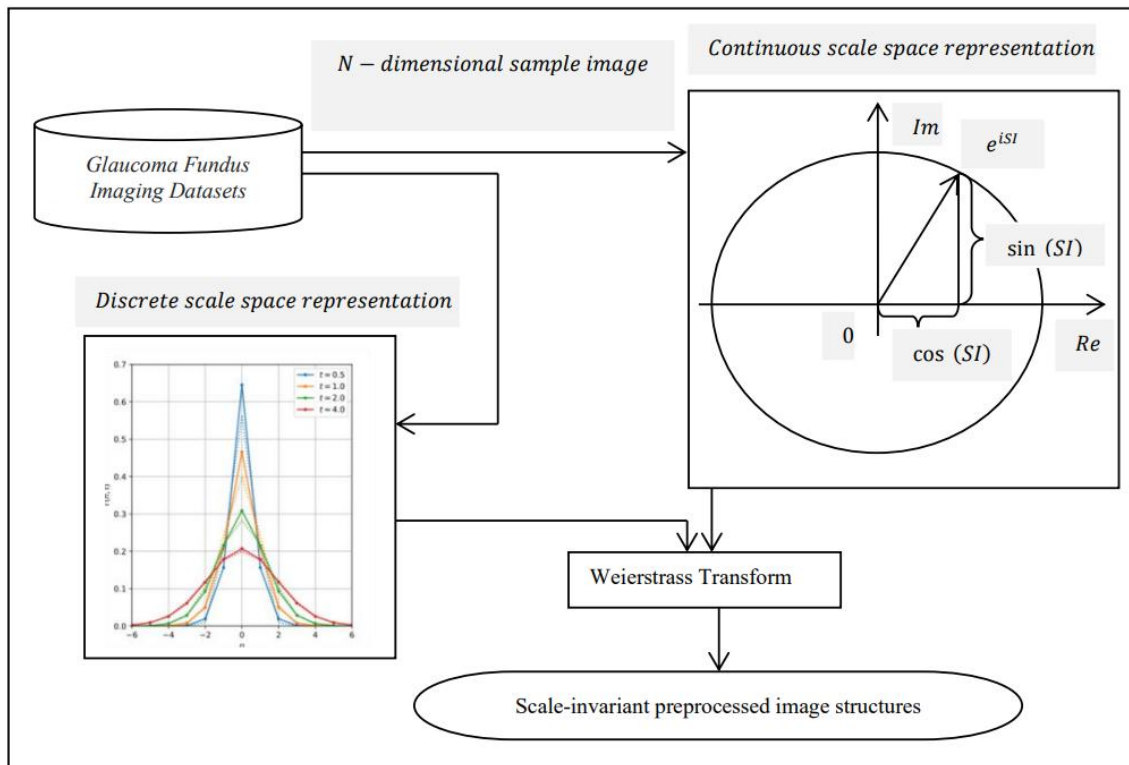


Figure 2. Structure of Weierstrass transform scale space representation-based preprocessing model

As illustrated in the Figure 2, let us consider the raw images obtained from the glaucoma fundus imaging datasets. The input images as illustrated in Figure 2 are subjected separately to discrete and continuous scale space representations. Finally, the values are averaged using Weierstrass transform function therefore forming scale-invariant preprocessed image structures as output. Let us consider a gaussian SSR of  $N$ -dimensional sample image represented as (1) and (2).

$$f_{C,D}(SI_1, SI_2, \dots, SI_n, t) \quad (1)$$

$$G_{C,D}(SI_1, SI_2, \dots, SI_n, t) \quad (2)$$

From the (1) and (2) gaussian scale space representation of a sample image 'SI' is obtained by convolving both the continuous and discrete representation of images ' $f_{C,D}$ ' based on the scale parameter 't'. As the (1) and (2) though formulated both for continuous and discrete forms of image representations however in practicality is not possible to apply similar scale space for both types of image representations. Hence, based on the separability characteristics of gaussian SSR, discrete and continuous representation of images of image structures at different scales is formulated as (3) to (5).

$$CSS(SI, t) = \sum f(SI - n)G(n, t) \tag{3}$$

$$G(n, t) = \sum_{i=1}^n \frac{1}{\sqrt{2\pi t}} e^{iSI} \tag{4}$$

$$e^{iSI} = \cos(SI) + i \sin(SI) \tag{5}$$

From the (3) and (4), using Euler’s identity obtained from (5) truncates at the end to generate a filtered result with finite impulse response therefore generating continuous scale space representation results.

$$DSS(SI, t) = \sum f(SI - n)T(n, t) \tag{6}$$

$$T(n, t) = e^{iSI} B_n(t) \tag{7}$$

$$B_n(t) = a^2 \frac{d^2b}{da^2} + a \frac{db}{da} + (a^2 - a)b = 0 \tag{8}$$

From the (6) and (7), using the Bessel function obtained from (8) for discrete scale space representation. Weierstrass transform function is applied to average the values of continuous scale space and discrete SSR results. This is formulated as (9).

$$PR = WTF(SI) = \frac{1}{\sqrt{4\pi}} \int_{-\infty}^{+\infty} f(y) e^{-\frac{(SI-y)^2}{4}} dy, \text{ where } y = CSS(SI, t).DSS(SI, t) \tag{9}$$

From the results (9) image structures at different scales are enhanced therefore ensuring the accuracy of ROI detection in extensive way.

Algorithm 1 describes the step-by-step process of Weierstrass transform scale space representation-based preprocessing. In the algorithm, through sample image obtained from the raw glaucoma fundus imaging dataset gaussian SSR of ‘N-dimension’ sample image is initially formulated. Second, continuous SSR and discrete SSR via Euler’s identity and Weierstrass transform function separately. Finally, both the scale representation results are combined to obtain preprocessed results that in turn ensure the accuracy of ROI detection in a significant manner.

**Algorithm 1.** Weierstrass transform scale space representation-based preprocessing

```

Input: Dataset ‘DS’, Sample Image ‘SI = {SI1, SI2, ..., SIn}’
Output: scale space-efficient preprocessed results ‘PR’
1: Initialize ‘n’, scale parameter ‘t’
2: Begin
3: For each Dataset ‘DS’ with Sample Image ‘SI’
4: Formulate Gaussian Scale Space Representation of an N-dimensional sample image as given in equations (1) and (2)
5: Measure continuous scale space representation results as given in equations (3), (4) and (5)
6: Measure discrete scale space representation results as given in equations (6), (7) and (8)
7: Generate preprocessed results by applying Weierstrass Transform function as given in equation (9)
8: Return preprocessed results ‘PR’
9: End for
10: End
    
```

**3.2. Composite dilated U-net convolution-based segmentation**

Segmentation of retinal blood vessels is regarded as an efficient mechanism for diagnosing ocular diseases to large extent glaucoma disease detection. Segmentation of blood vessels is performed by employing CDC model. Here segmentation is performed for the preprocessed sample input image to identify glaucoma by the CDC evaluation. With the preprocessed image results as input, automatic optic disc as well as cup segmentation depend on DL such as CDC model is designed. By using CDC model edge features are retained and also image diagnostic error is improved by means of log cosh dice loss function. The block diagram of the CDC-based segmentation model is described in Figure 3.

Figure 3 demonstrates the block diagram of the CDC-based segmentation model. This model includes input layer, hidden layer, and output layer. At first, the preprocessed sample input image (i.e., preprocessed result ‘PR’) is taken through the convolutional layer. Moreover, FReLU activation is utilized in hidden layer whereas the sigmoid function is used to output layer. Two processes are carried out such as log

cosh dice loss function and optic cup to disc ratio in the output layer. The glaucoma diagnosis is made in an accurate manner.

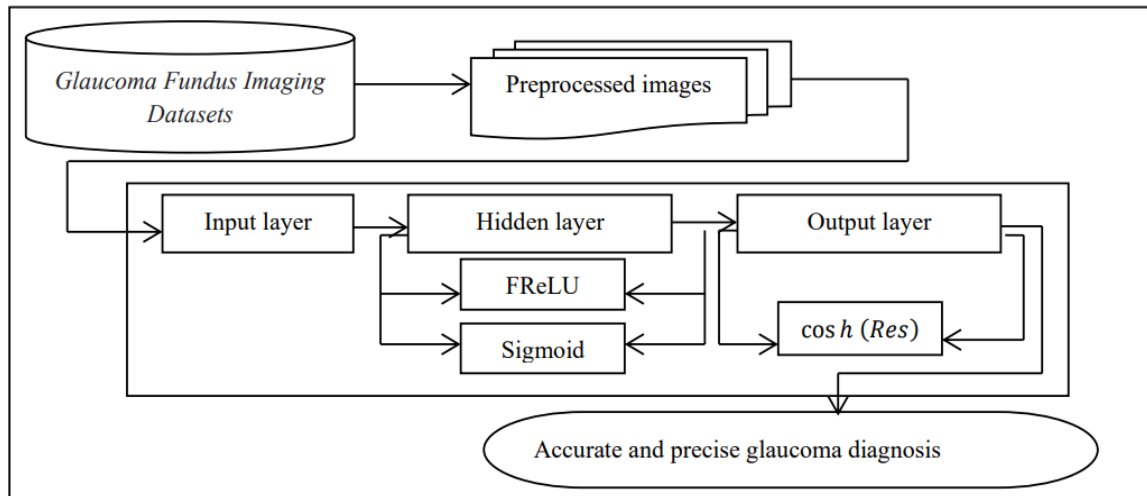


Figure 3. Block diagram of CDC-based segmentation model

FReLU being a linear function with the input being positive, the output value is the same as the input value. On contrary, the output of zero is produced and is mathematically expressed as (10).

$$R_1(PR) = \max(0, PR) \quad (10)$$

From the (10), 'PR' forms the input or the preprocessed results provided as input. Then, the above function satisfying duality condition is stated as (11).

$$R_1(SI) = \begin{cases} SI, & \text{if } SI > 0 \\ 0, & \text{if } SI \leq 0 \end{cases} \quad (11)$$

This architecture included two paths, namely, contracting path and expansion path respectively. Both of them applied the FReLU as the activation function. By applying this function has the advantage of determining the segmented portions in an accurate and precise manner for glaucoma detection. On one hand, the feature extraction is performed by the contracting path whereas the segmentation mapped results are obtained by synthesizing the spatial information with high resolution features. In contracting path, two convolution layers of '3 × 3' are repeated.

Moreover, maxpooling of '2 × 2' is carried out. In each step in constricting path, number of aspect channels is enhanced moderately from '16 to 256'. Conversely, in the expansion path, the number of feature channels is reduced from '256 to 16'. Additionally, the maxpooling layer of '2 × 2' and two convolution layers of '3 × 3' are performed consecutively. Next, the fragment derivative for preprocessed result for the first derivative, second derivative '2' and 'n - th' derivative to increase the resolution of the outputs via composite dilation is stated as (11) to (13).

$$f(SI) = SI^k \rightarrow Df(SI) = \frac{d}{dSI} f(SI) = kSI^{k-1} \quad (11)$$

$$D^2 f(SI) \frac{d^2}{dSI^2} f(SI) = k(k-1)SI^{k-2} \quad (12)$$

$$D^n f(SI) \frac{d^n}{dSI^n} f(SI) = k(k-1)SI^{k-n} \quad (13)$$

Then the FReLU is stated as (14).

$$Res = FReLU = \begin{cases} \frac{k!}{(k-n)!} SI^{k-n}; & \text{if } SI > 0 \\ 0; & \text{if } SI \leq 0 \end{cases} \quad (14)$$

Next, with obtained activation results in hidden layer via 'Res' as provided (14), to obtain higher segmentation performance results, log cosh dice loss function is formulated as (15).

$$\cosh(Res) = \log \cos \left( \frac{e^{Res} + e^{-Res}}{2} \right) \quad (15)$$

Finally, the most extensively utilized measured for glaucoma detection, namely, using optic CDR is most widely used feature for glaucoma detection. The reason behind the employment of CDR is that the phenomenon of cupping is said to occur upon prevalence of certain considerable amount of strain churned out in the retina. The CDR here is measured taking into considerations the area of OC and OD. It mathematically formulated as (16).

$$CDR = 2 * \left[ \frac{Area_{cup}[Res]}{Area_{disc}[Res]} \right] \quad (16)$$

From (16) CDR is formulated depend on area of cup 'Area<sub>cup</sub>' and area of disc 'Area<sub>disc</sub>' with respect to the resultant images obtained in 'Res' respectively. According to the resultant values obtained in (16), the output in the output layer is generated by either glaucomatous or healthy image results. The pseudo code representation of CDC-based segmentation is given in Algorithm 2.

**Algorithm 2.** CDC-based segmentation for glaucoma detection

```

Input: Dataset 'DS'
Output: Early glaucoma detection
1: Initialize 'n', preprocessed results 'PR'
2: Begin
3: For each Dataset 'DS' with preprocessed results 'PR'
//Input layer
4: Provide preprocessed results 'PR' as input
//Hidden layer
5: Formulate ReLU activation for each preprocessed results 'PR' as given in equations (10)
and (11)
6: Formulate fragment derivative for preprocessed result as given in equations (11), (12)
and (13)
7: Formulate FReLU activation function as given in equation (14)
//Output layer
8: Measure log cosh dice loss function as given in equation (15)
9: Measure optic cup to disc ratio as given in equation (16)
10: If 'Val[CDR] ≥ 0.5'
11: Then glaucomatous image
12: End if
13: If 'Val[CDR] < 0.5'
14: Then healthy image
15: End for
16: End

```

The CDC-based segmentation is illustrated in Algorithm 2. As given in algorithm 2, to ensure early glaucoma detection with minimal error, first, the preprocessed input images are given as input to the input layer. Second, in hidden layer fragment derivative for each preprocessed input are obtained. Lastly, in the output layer two processes are carried out, first, log cosh dice loss function is applied to reduce the diagnostic error and then optic CDR is evaluated to obtain the segmented glaucoma detected results in an accurate and precise manner.

#### 4. RESULTS AND DISCUSSION

The proposed WSSR-CDC for glaucoma detection is evaluated using Python high-level programming-language and results are compared with the previous works such as, multi-feature MFDL [1] and multi-task DL [2]. The aim of the proposed WSSR-CDC is to achieve accurate glaucoma detection with maximum accuracy and lesser diagnostic error. Based on the objective, the existing methods such as MFDL [1] and multi-task DL [2] are taken as base paper. These two base papers are explained to understand the proposed method. The existing DL methods were designed for glaucoma detection. However, the accuracy was not enhanced, diagnostic error was not reduced. The proposed method concept is derived by considering

the problems of these base papers. The drawbacks of these methods are effectively convinced by implementing the proposed method. In addition, the results are evaluated based on the metrics such as sensitivity, specificity, image diagnostic error and accuracy using the glaucoma fundus imaging dataset extracted from <https://www.kaggle.com/datasets/arnavjain1/glaucoma-datasets>. The performance of the WSSR-CDC method is compared with the other competing methods, MFDL [1] and multi-task DL [2] and validated.

#### 4.1. Implementation details

We developed an early glaucoma detection method called WSSR-CDC with improved precision and accuracy:

- The WSSR-CDC method comprises two sections, namely, preprocessing and segmentation.
- The WSSR-CDC method is compared with two existing methods, MFDL [1] and multi-task DL [2] using a glaucoma fundus imaging dataset to validate the results.
- Initially, the fundus images are obtained as input from the dataset. The images were subjected to preprocessing and segmentation for early glaucoma detection.
- In the first part, the Weierstrass transform scale space representation-based preprocessing model is employed to process image structures at different scales via Euler's identity.
- Second, a DL model employing CDC model is utilized to preprocessed noise image. The process undergoes contracting and expansion separately. Also to minimize diagnostic error, log cosh dice loss function is applied. Finally, using optic CDR glaucoma detection is made in extensive manner.

According to the above implementation patterns, four different evaluation metrics are detailed in the next section.

#### 4.2. Discussion

First, sensitivity test is performed to measure its ability to determine the patient cases correctly (i.e., glaucoma as glaucoma and healthy as healthy). To measure the sensitivity, rate the proportion or ratio of true positive in-patient cases has to be analyzed. To be more specific, sensitivity indicates the ratio of positives which are properly hypothesized. It is expressed as (17).

$$Sensitivity = \frac{TP}{TP+FN} \quad (17)$$

From the (17), sensitivity rate '*Sensitivity*', is calculated depend on true positive cases '*TP*' (i.e., healthy patient detected as healthy) as well as false negative cases '*FN*' (i.e., healthy patient detected as glaucoma) respectively. Second, specificity or the probability of negative test results is evaluated. Specificity indicates the fraction of negatives that are accurately inferred and expressed as (18).

$$Specificity = \frac{TN}{TN+FP} \quad (18)$$

From (18), specificity '*Specificity*', rate is calculated, depend on true negative rate '*TN*' (i.e., glaucoma patient detected as glaucoma) and the false positive '*FP*' (i.e., glaucoma patient detected as healthy) rate respectively. Third, for assessing the significance of glaucoma detection one of the important performance metrics is accuracy. Accuracy is referred the ratio of proper forecast to total number of samples. It is formulated as (19).

$$Acc = \frac{TP+TN}{TP+TN+FP+FN} \quad (19)$$

From the (19), accuracy rate '*Acc*', is estimated by true positive rate '*TP*', *TN*, false positive rate *FP* and *FN*. It is calculated in percentage (%). Finally, diagnostic error or measure to validate the effectiveness of technique is formulated as (20).

$$DiagErr = \sum_{i=1}^n \frac{S_{WD}}{S_i} * 100 \quad (20)$$

From the (20), the diagnostic error '*DiagErr*' is evaluated by samples '*S<sub>i</sub>*' as well as samples wrongly detected '*S<sub>WD</sub>*' with healthy as glaucoma and glaucoma as healthy.

Table 1 compares the outcomes of the WSSR-CDC technique of sensitivity with those other methods, MFDL [1] and multi-task DL [2] using the glaucoma fundus imaging dataset. The reason for

enhancing the sensitivity is to apply gaussian scale space representation. Here, the discrete and continuous representation of image structures at different scales was obtained using Euler's identity and Bessel function. This in turn improved the overall sensitivity of WSSR-CDC technique by 12% and 24% than the [1], [2].

Figure 4 illustrates a graphical depiction of specificity for 2,000 different sample images provided as input. Finally, continuous scale space and discrete scale space representations were combined using Weierstrass transform function that in turn ensures accuracy of ROI detection in a significant manner and therefore improving the specificity using WSSR-CDC technique by 8% and 14% than the [1], [2].

Table 2 compares the outcomes of the proposed WSSR-CDC method in terms of accuracy with those other methods, MFDL [1] and multi-task DL [2] using the glaucoma fundus imaging dataset. The two different activation functions are utilized in the hidden layer. The first activation function was the employment of FReLU where with the preprocessed result images as input, the fragment derivative for the first derivative was obtained and the second derivative was measured. Finally, 'n - th' derivative was formulated with the purpose of increasing the resolution of the outputs via composite dilation. This in turn reduced FP and FN rate and therefore improving overall accuracy of WSSR-CDC method by 8% upon comparison to [1] and 16% upon comparison to [2].

Table 1. Comparison of the performance of sensitivity of WSSR-CDC method with existing MFDL [1] and multi-task DL [2]

Sample images	Sensitivity		
	WSSR-CDC	MFDL	multi-task DL
200	0.9	0.84	0.77
400	0.87	0.82	0.74
600	0.85	0.8	0.71
800	0.84	0.78	0.69
1,000	0.83	0.75	0.66
1,200	0.81	0.73	0.63
1,400	0.78	0.7	0.6
1,600	0.78	0.7	0.6
1,800	0.82	0.72	0.65
2,000	0.83	0.74	0.67

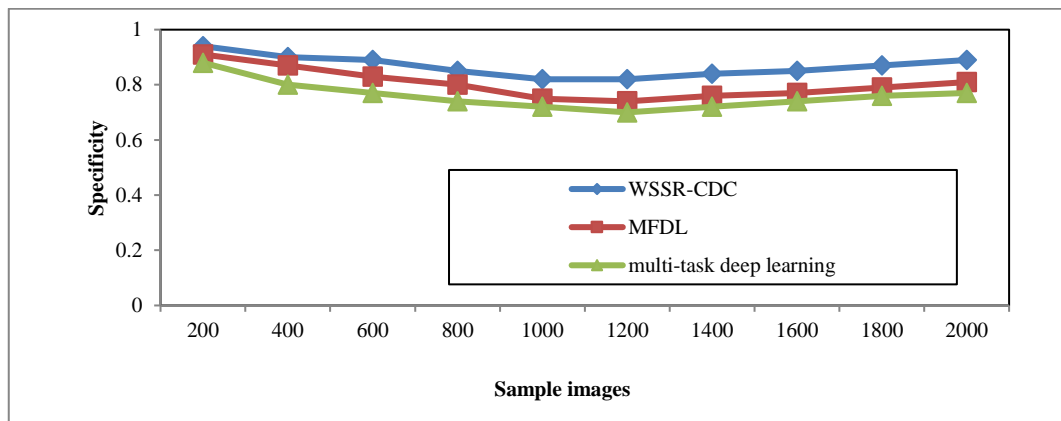


Figure 4. Specificity versus sample images

Table 2. Comparison of accuracy of the WSSR-CDC method, MFDL [1] and multi-task DL [2]

Sample images	Accuracy (%)		
	WSSR-CDC	MFDL	multi-task DL
200	0.94	0.88	0.83
400	0.92	0.84	0.81
600	0.88	0.82	0.78
800	0.85	0.81	0.75
1,000	0.83	0.78	0.71
1,200	0.82	0.75	0.69
1,400	0.82	0.75	0.69
1,600	0.84	0.77	0.71
1,800	0.86	0.79	0.73
2,000	0.88	0.81	0.75

Figure 5 depicts a graphical depiction of the error rate when substituted in (20) for three methods WSSR-CDC, MFDL [1], and multi-task DL [2]. The reason was that by applying the log cosh dice loss function higher segmentation performance results were obtained. Next, based on the optic CDR segmented portions were analyzed for glaucoma and healthy images. This in turn reduced the wrongly detected results and therefore reduced the overall diagnostic error using the WSSR-CDC method by 26% and 37% than the [2].

The early stage of glaucoma identification is a crucial task to avoid blindness. Most convolution techniques are developed to determine eye disorders through fundus images. The existing methods are described in the major issues such as lesser accuracy, higher error, minimum sensitivity, the glaucoma identification performance was not improved, and failure to provide accurate results. To overcome the issues, in order to solve this issue, a novel WSSR-CDC method is needed for early disease detection. The major findings and outcome of the proposed WSSR-CDC method observed from the above results are as follows:

- The proposed method addresses the early glaucoma detection in retinal fundus images by using Weierstrass transform scale space representation and CDC model.
- The proposed method uses the Weierstrass transform scale space representation for performing preprocessing to create generate scale-invariant preprocessed images with higher sensitivity.
- The proposed method employs CDC model for identifying to detecting glaucoma.
- Log cosh dice loss function is utilized to decrease the diagnostic error.
- The optic cup to disc ratio is measured to get the segmented glaucoma detected results.
- The outcome of the proposed method achieves 24% of accuracy, 18% of sensitivity, 11% of specificity, and 32% of error as compared to existing works.

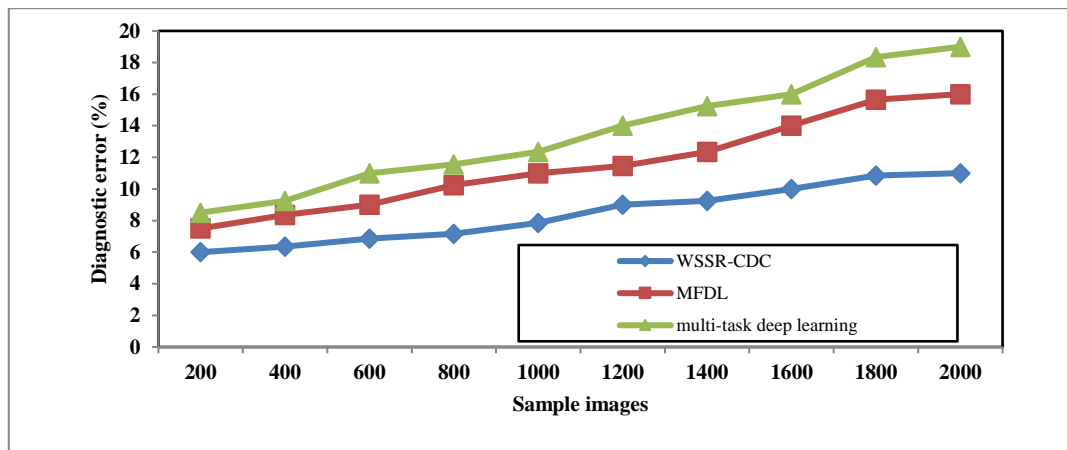


Figure 5. Diagnostic errors versus sample images

## 5. CONCLUSION

In our work, the objective of the proposed WSSR-CDC for glaucoma detection using glaucoma fundus retinal images is to obtain accurate and precise glaucoma detected results. First, preprocessing using raw images was performed using Weierstrass transform scale space representation to obtain processed results at different scales. Next, with the preprocessed image results, segmentation for glaucoma detection was performed by means of CDC model. Here also composite dilated results were subjected to log cosh dice loss function with the objective of retaining the edge features with minimal diagnostic error. By incorporating these features into FReLU, excellent segmentation accuracy was achieved compared to preceding techniques. The proposed WSSR-CDC is to provide precise glaucoma results employing Weierstrass transform scale space representation based preprocessing model and CDC model for segmentation with minimum error and maximum accuracy and specificity. These findings have implications for identifying the glaucoma.

Experiments were performed on the glaucoma fundus retinal image database to test the performance of the proposed technique and existing methods. The proposed WSSR-CDC is compared with the two existing methods (i.e. MFDL and multi-task DL). The results of the WSSR-CDC provide better performance with an improvement of accuracy by 24%, sensitivity by 18% specificity by 11%, and reduction of error by 32% as compared to existing works. The proposed WSSR-CDC method achieves better accuracy and sensitivity with minimal diagnostic error than the conventional methods. In future work, the proposed method is further extended to use new research work for detecting the glaucoma results by using various convolution techniques. In addition, the feature selection is performed to extract the features with less time.

**FUNDING INFORMATION**

There is no funding agency.

**AUTHOR CONTRIBUTIONS STATEMENT**

Name of Author	C	M	So	Va	Fo	I	R	D	O	E	Vi	Su	P	Fu
Abdul Basith Zahir Hussain	✓	✓	✓	✓	✓	✓	✓		✓	✓	✓	✓	✓	
Sulthan Ibrahim Mohamed Sulaiman	✓	✓	✓	✓	✓	✓	✓	✓	✓	✓	✓	✓	✓	

C : **C**onceptualization

M : **M**ethodology

So : **S**oftware

Va : **V**alidation

Fo : **F**ormal analysis

I : **I**nvestigation

R : **R**esources

D : **D**ata Curation

O : Writing - **O**riginal Draft

E : Writing - Review & **E**ditng

Vi : **V**isualization

Su : **S**upervision

P : **P**roject administration

Fu : **F**unding acquisition

**CONFLICT OF INTEREST STATEMENT**

We have no conflicts of interest related to this work.

**INFORMED CONSENT**

Informed consent was obtained from all participants involved in this study. The participants were provided with comprehensive information regarding the study’s objectives, procedures, potential risks, and benefits before giving their consent. We acknowledge Mr. Abdul Basith Z and Dr. Sulthan Ibrahim M for their contributions in obtaining and ensuring proper documentation of informed consent from all individuals involved in the study.

**DATA AVAILABILITY**

The data that support the findings of this study are openly available in [www.kaggle.com](http://www.kaggle.com)

- The data that support the findings of this study will be available in [[www.kaggle.com](http://www.kaggle.com)] [<https://www.kaggle.com/datasets/arnavjain1/glaucoma-datasets>].

The data that support the findings of this study are available on request from the corresponding author, Abdul Basith Zahir Hussain

- The data, which contain information that could compromise the privacy of research participants, are not publicly available due to certain restrictions.
- Derived data supporting the findings of this study are available from the corresponding author z on request.
- The data that support the findings of this study are available from No third party
- Restrictions apply to the availability of these data, which were used under license for this study. Data are available [doi: 10.1016/j.jbi.2022.104233]
- The authors confirm that the data supporting the findings of this study are available within the article
- The data that support the findings of this study are available from the corresponding author, Author initial Z upon reasonable request.
- Data availability is not applicable to this paper as no new data were created or analysed in this study.

**REFERENCES**

- [1] Y. Xue *et al.*, “A multi-feature deep learning system to enhance glaucoma severity diagnosis with high accuracy and fast speed,” *Journal of Biomedical Informatics*, vol. 136, p. 104233, Dec. 2022, doi: 10.1016/j.jbi.2022.104233.
- [2] L. Pascal, O. J. Perdomo, X. Bost, B. Huet, S. Otálora, and M. A. Zuluaga, “Multi-task deep learning for glaucoma detection from color fundus images,” *Scientific Reports*, vol. 12, no. 1, p. 12361, Jul. 2022, doi: 10.1038/s41598-022-16262-8.
- [3] J.-A. Kim *et al.*, “Development of a deep learning system to detect glaucoma using macular vertical optical coherence tomography scans of myopic eyes,” *Scientific Reports*, vol. 13, no. 1, p. 8040, May 2023, doi: 10.1038/s41598-023-34794-5.
- [4] S. Saha, J. Vignarajan, and S. Frost, “A fast and fully automated system for glaucoma detection using color fundus photographs,” *Scientific Reports*, vol. 13, no. 1, p. 18408, Oct. 2023, doi: 10.1038/s41598-023-44473-0.
- [5] J. Latif, S. Tu, C. Xiao, S. Ur Rehman, A. Imran, and Y. Latif, “ODGNet: a deep learning model for automated optic disc localization and glaucoma classification using fundus images,” *SN Applied Sciences*, vol. 4, no. 4, p. 98, Apr. 2022, doi: 10.1007/s42452-022-04984-3.

- [6] M. Yan, Y. Lin, X. Peng, and Z. Zeng, "mixDA: mixup domain adaptation for glaucoma detection on fundus images," *Neural Computing and Applications*, pp. 1–20, Jul. 2023, doi: 10.1007/s00521-023-08572-3.
- [7] R. Thanki, "A deep neural network and machine learning approach for retinal fundus image classification," *Healthcare Analytics*, vol. 3, p. 100140, Nov. 2023, doi: 10.1016/j.health.2023.100140.
- [8] V. K. Velpula and L. D. Sharma, "Multi-stage glaucoma classification using pre-trained convolutional neural networks and voting-based classifier fusion," *Frontiers in Physiology*, vol. 14, p. 1175881, Jun. 2023, doi: 10.3389/fphys.2023.1175881.
- [9] S. Ajitha, J. D. Akkara, and M. V. Judy, "Identification of glaucoma from fundus images using deep learning techniques," *Indian Journal of Ophthalmology*, vol. 69, no. 10, pp. 2702–2709, Oct. 2021, doi: 10.4103/ijo.IJO\_92\_21.
- [10] L. K. Singh, Pooja, H. Garg, and M. Khanna, "Performance evaluation of various deep learning based models for effective glaucoma evaluation using optical coherence tomography images," *Multimedia Tools and Applications*, vol. 81, no. 19, pp. 27737–27781, Aug. 2022, doi: 10.1007/s11042-022-12826-y.
- [11] X. Xu, Y. Guan, J. Li, Z. Ma, L. Zhang, and L. Li, "Automatic glaucoma detection based on transfer induced attention network," *BioMedical Engineering OnLine*, vol. 20, no. 1, p. 39, Dec. 2021, doi: 10.1186/s12938-021-00877-5.
- [12] G. D'Souza, P. C. Siddalingaswamy, and M. A. Pandya, "AlterNet-K: a small and compact model for the detection of glaucoma," *Biomedical Engineering Letters*, vol. 14, no. 1, pp. 23–33, Jan. 2024, doi: 10.1007/s13534-023-00307-6.
- [13] S. Pathan, P. Kumar, R. M. Pai, and S. V. Bhandary, "An automated classification framework for glaucoma detection in fundus images using ensemble of dynamic selection methods," *Progress in Artificial Intelligence*, vol. 12, no. 3, pp. 287–301, Sep. 2023, doi: 10.1007/s13748-023-00304-x.
- [14] S. Gheisari *et al.*, "A combined convolutional and recurrent neural network for enhanced glaucoma detection," *Scientific Reports*, vol. 11, no. 1, p. 1945, Jan. 2021, doi: 10.1038/s41598-021-81554-4.
- [15] A. K. Schuster, C. Erb, E. M. Hoffmann, T. Dietlein, and N. Pfeiffer, "The diagnosis and treatment of glaucoma," *Deutsches Arzteblatt International*, vol. 117, no. 13, pp. 225–234, Mar. 2020, doi: 10.3238/arztebl.2020.0225.
- [16] S. Vilakkumadathil and V. Thiyagarajan, "Exploring diverse prediction models in intelligent traffic controls," *Indonesian Journal of Electrical Engineering and Computer Science*, vol. 38, No. 1, pp. 393–402, 2025, doi: 10.11591/ijeecs.v38.i1.pp393-402.
- [17] A. Sevastopolsky, "Optic disc and cup segmentation methods for glaucoma detection with modification of U-Net convolutional neural network," *Pattern Recognition and Image Analysis*, vol. 27, no. 3, pp. 618–624, 2017, doi: 10.1134/S1054661817030269.
- [18] F. Du *et al.*, "Recognition of eye diseases based on deep neural networks for transfer learning and improved D-S evidence theory," *BMC Medical Imaging*, vol. 24, no. 1, p. 19, Jan. 2024, doi: 10.1186/s12880-023-01176-2.
- [19] N. Akter, J. Fletcher, S. Perry, M. P. Simunovic, N. Briggs, and M. Roy, "Glaucoma diagnosis using multi-feature analysis and a deep learning technique," *Scientific Reports*, vol. 12, no. 1, p. 8064, May 2022, doi: 10.1038/s41598-022-12147-y.
- [20] M. S. Puchaicela-Lozano *et al.*, "Deep learning for glaucoma detection: R-CNN ResNet-50 and image segmentation," *Journal of Advances in Information Technology*, vol. 14, no. 6, pp. 1186–1197, 2023, doi: 10.12720/jait.14.6.1186-1197.
- [21] V. Haja, S. A. Mahadevappa, "Advancing glaucoma detection with convolutional neural networks: a paradigm shift in ophthalmology," *Romanian Journal of Ophthalmology*, vol. 67, no. 3, pp. 222–237, Nov. 2023, doi: 10.22336/rjo.2023.39.
- [22] R. Mahum, S. U. Rehman, O. D. Okon, A. Alabrah, T. Meraj, and H. T. Rauf, "A novel hybrid approach based on deep CNN to detect glaucoma using fundus imaging," *Electronics*, vol. 11, no. 1, p. 26, Dec. 2021, doi: 10.3390/electronics11010026.
- [23] X. Huang *et al.*, "Artificial intelligence in glaucoma: opportunities, challenges, and future directions," *BioMedical Engineering OnLine*, vol. 22, no. 1, p. 126, Dec. 2023, doi: 10.1186/s12938-023-01187-8.
- [24] M. Lin *et al.*, "Automated diagnosing primary open-angle glaucoma from fundus image by simulating human's grading with deep learning," *Scientific Reports*, vol. 12, no. 1, p. 14080, Aug. 2022, doi: 10.1038/s41598-022-17753-4.
- [25] Y. Li, Y. Han, Z. Li, Y. Zhong, and Z. Guo, "A transfer learning-based multimodal neural network combining metadata and multiple medical images for glaucoma type diagnosis," *Scientific Reports*, vol. 13, no. 1, p. 12076, Jul. 2023, doi: 10.1038/s41598-022-27045-6.

## BIOGRAPHIES OF AUTHORS



**Abdul Basith Zahir Hussain**    received the B.Sc. degree in computer science from the Jamal Mohamed College, affiliated to the Bharadhidasan University, Tamil Nadu, India, the M.Sc. degree in computer science from the Vels University, Chennai, India, the M.Phil. degree in computer science from the Gandhigram Rural Institute, Tamil Nadu, India and pursuing the Ph.D. degree in computer science in the Madurai Kamaraj University, Madurai, India. He is currently an assistant professor with the department of information technology, Hajee Karutha Rowther Howdia College, Tamil Nadu, India. He has 7 years of teaching experience. He can be contacted at email: abdbasith93@gmail.com.



**Dr. Sulthan Ibrahim Mohamed Sulaiman**    is an associate professor and head of the department in department of computer science, Government Arts and Science College, Veerapandi, Theni, Tamil Nadu, India since June 2016. He pursued master of philosophy in computer science from Madurai Kamaraj university, India in 2004 and doctor of philosophy from Bharathidasan University in year 2016. His main research work focuses on data mining, web mining, cryptography and network security, IoT and artificial intelligence-based education. He has published research paper in various international journals and conferences. He serves as doctoral committee members of the various universities. He has 25 years of teaching experience and more than 16 years of research experience. He can be contacted at email: km.sulthan@gmail.com.